ACS APPLIED MATERIALS & INTERFACES

www.acsami.org
Research Article

PEDOT:PSS Wire: A Two-Terminal Synaptic Device for Operation in Electrolyte and Saline Solutions

Seiya Watanabe,* Hiroaki Shibakita, Naruki Hagiwara, Ryosuke Nakajima, Hiroyuki S. Kato, and Megumi Akai-Kasaya

Cite This: *ACS Appl. Mater. Interfaces* 2024, 16, 54636−54644

ABSTRACT: Synaptic devices, which are designed to emulate the synaptic functions of neurons, have recently gained attention as key elements in the development of neuromorphic hardware. To date, most synaptic devices utilizing conductive polymer materials, particularly poly(3,4-ethylenedioxythiophene):poly(styrenesulfonate) (PEDOT:PSS), have been designed as three-terminal devices. Nevertheless, a recent study revealed that a single PEDOT:PSS wire can function as a two-terminal synaptic device through additional polymerization, which creates asymmetry in the wire diameter between the anode and cathode. Owing to its high biocompatibility, PEDOT is considered a promising candidate for use in clinical information-processing devices. However, previous studies examined the synaptic function of PEDOT:PSS only in PSS solutions. Therefore, the performance of PEDOT:PSS wires in other solutions, such as physiological saline solutions, remains unknown. Herein, we investigated the effects of operating environmental conditions (including phosphate-buffered saline (PBS)) on the synaptic functions of the asymmetric PEDOT:PSS wire. Our results indicate that the synaptic conductance change in the PEDOT:PSS wire occurred in all investigated aqueous electrolyte solutions. Moreover, we revealed the relationship between the synaptic conductance change behavior and the molecular properties of the electrolyte ions. Furthermore, the waveform of the conductance change can be controlled by adjusting the conditions for wire asymmetrization. These results demonstrate that the PEDOT:PSS wire exhibits a synaptic conductance change, yielding a waveform suitable for machine learning, even under wet conditions (i.e., in any electrolyte solution, including PBS). Therefore, PEDOT:PSS wire is a promising material for two-terminal synaptic devices applicable in clinical studies.

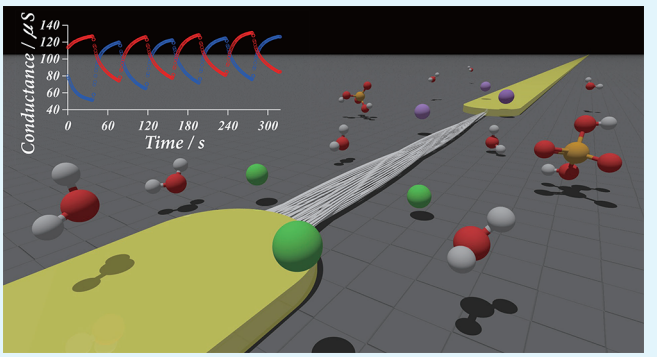

KEYWORDS: *synaptic device, conductive polymer, polymer wire, neuromorphic, clinical application*

INTRODUCTION

The rapid development of artificial intelligence (AI) technology has accelerated power consumption. In contrast to AI, the human brain exhibits sophisticated information-processing capabilities while consuming an extremely low amount of power. To address the energy-intensive nature of AI, researchers have been studying neuromorphic hardware, a computing architecture imitating the cranial nervous system.[1,2] A crucial component in developing such hardware is the synaptic device, designed to replicate the synaptic function of neurons in neural circuits. Developing a functional synaptic device requires the incorporation of nonvolatile variable-resistance properties, which has prompted extensive research into various materials.[3−5] Although most research on synaptic devices has focused on solid-state devices, namely, memristors, synaptic devices made of conductive polymers have lately attracted attention because of their advantages of low power consumption and flexibility.[6−8] Van de Burgt et al. developed a poly(3,4-ethylenedioxythiophene):poly(styrenesulfonate) (PEDOT:PSS) electrolyte transistor device that exhibits lower power consumption and a wider resistance range than existing inorganic memristors.[6] PEDOT, a biocompatible material already used in sensors[9,10] and actuators[11] that operate *in vivo*, holds promise for use in synaptic devices for information processing in clinical applications. Most PEDOT-based synaptic devices reported in previous studies were three-terminal devices. However, Hagiwara et al. recently reported that a single PEDOT:PSS polymer wire can function as a two-terminal synaptic device through a specific fabrication process.[12] The procedure involved growing a PEDOT:PSS wire using alternating current (AC) voltage in a solution of 3,4-

Received: July 19, 2024
Revised: September 6, 2024
Accepted: September 20, 2024
Published: September 30, 2024

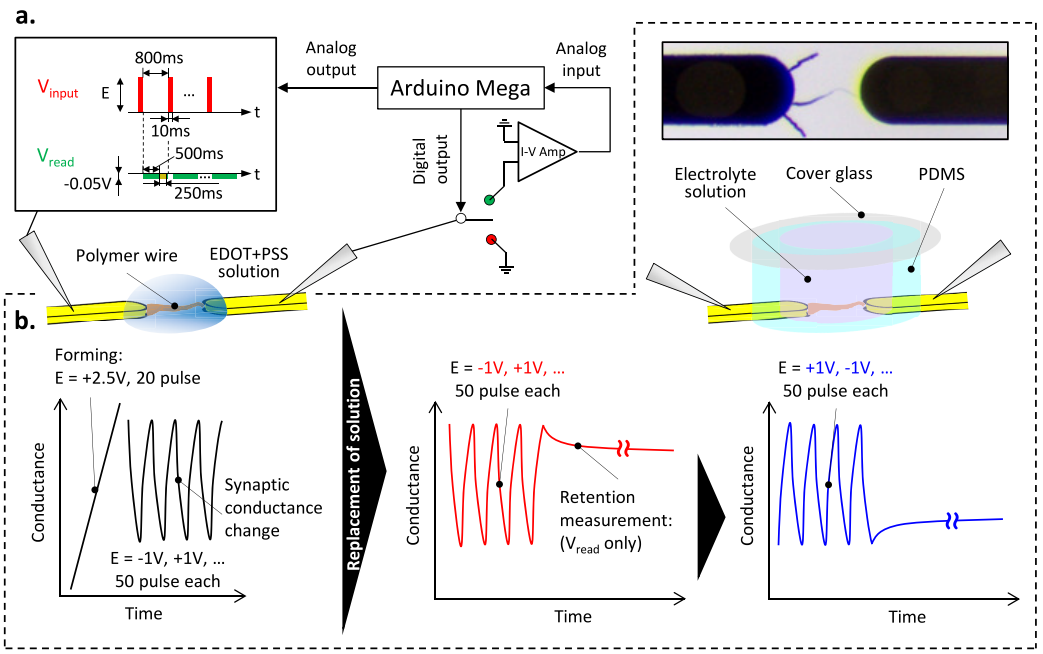

Figure 1. Schematic of (a) experimental setups and (b) method of fabricating and evaluating a synaptic PEDOT:PSS wire.

ethylenedioxythiophene (EDOT) and PSS and then cross-linking it between electrodes. Subsequently, the diameter of the wire near the anode was increased by applying pulses of direct current (DC) voltage above the electrolytic polymerization potential. The PEDOT:PSS wire fabricated in this manner had different anode and cathode diameters and exhibited conductance changes upon application of DC pulses below the electrolytic polymerization potential. The direction of conductance change (i.e., increase or decrease) depended on the polarity of the applied voltage. Therefore, the conductance could be changed continuously and plastically in both directions by controlling the polarity, magnitude, and number of applied voltage pulses. The asymmetric wire diameters caused differences in the doping and dedoping reaction efficiencies at the anode and cathode, respectively.[12] In addition, PEDOT:PSS wire offers a high degree of wiring flexibility. Notably, neuromorphic networks based on three-dimensional PEDOT:PSS wiring have recently been achieved.[13] Although there have been several reports of two-terminal synaptic devices that operate in solution, PEDOT:PSS wire is a material with great advantages for integration. Therefore, the developed two-terminal synaptic device utilizing flexible PEDOT:PSS wire holds great promise for integrated synaptic device architectures.

In addition to their use in synaptic devices, PEDOT and PEDOT-based conductive polymers have been utilized in reservoir-computing devices. Reservoir computing is a learning framework comprising a reservoir, a recurrent neural network with sparse and randomly connected links, and a readout. Unlike conventional recurrent neural networks, in reservoir computing, only the weights of the readout are updated during the learning process, whereas the weight of the reservoir remains unchanged, enabling simple physical implementation and extremely fast learning with a low computational cost. The physical implementation of reservoir computing has led to the development of innovative devices capable of power-saving real-time processing and has thus been intensively studied. Cucchi et al. reported the successful classification of arrhythmias from pulsation patterns using a reservoir device constructed with a PEDOT:hexafluorophosphate (PF_6) wire network. Furthermore, they demonstrated the potential of using such devices as sensors wrapped around a finger;[14] owing to the biocompatibility of PEDOT, the prospect of embedding sensors inside the human body becomes feasible. Thus, PEDOT is a promising material for use in reservoir devices for clinical applications. However, the readout remains a challenge for the physical implementation of reservoir systems. Learning in a reservoir system involves adjusting the weights (w) of the readout; however, this readout calculation is typically executed using an external computer.[14−16] Embedding a conventional reservoir system requires vast memory to store the reservoir output information or involves high communication traffic for sequential processing, making it impractical for certain applications. Therefore, a desirable solution is to implement the reservoir and readout. An example of such a solution is embedding an entire reservoir system (reservoir and readout) with a communicator programmed to communicate when receiving a signal from the reservoir system that satisfies a prescribed condition, leading to the development of an intelligent system that communicates the required information only when necessary. Synaptic devices have emerged as potential candidates for performing calculations at the readout. Milano et al. demonstrated the successful physical implementation of a readout comprising a crossbar array based on TaO_x synaptic devices and a physical reservoir device.[17] However, for clinical applications, developing synaptic devices using biocompatible materials instead of metal oxides and/or chalcogenides is desirable.

Herein, we examine the potential of using a PEDOT:PSS wire as a biocompatible synaptic device. A previous study[12] revealed that an asymmetric PEDOT:PSS wire exhibited synaptic conductance changes in a mixture of monomer and dopant solutions (EDOT + PSS solutions) and in a dopant solution. However, its behavior in other solutions, such as physiological saline solutions, remains unclear. To this end, we investigated the synaptic conductance changes in PEDOT:PSS

https://doi.org/10.1021/acsami.4c12037
ACS Appl. Mater. Interfaces 2024, 16, 54636−54644

wires in various electrolyte solutions. Moreover, we analyzed and discussed the relationship between synaptic device properties (full switching window and retention characteristics) and molecular properties of electrolyte ions (ionic radius and chemical hardness (η)) using density functional theory (DFT), shedding light on the detailed contribution mechanism of electrolyte ions to synaptic conductance changes.

EXPERIMENTAL METHODS

Materials. A PEDOT:PSS wire was fabricated using a mixture of 0.135 M EDOT (>97%, Sigma-Aldrich, USA) and 0.02 M PSS (Mw = 75,000, Sigma-Aldrich, USA) solutions prepared in a 1:1 mixture of water and acetonitrile. As replacement solutions, we used 0.1 M aqueous solutions of five electrolytes: PSS, lithium perchlorate ($LiClO_4$: >99.99% trace metal basis, Sigma-Aldrich, St. Louis, Missaouri), and sodium *p*-toluenesulfonate (NaPTs: >90.0%, Tokyo Chemical Industry Co., Ltd., Japan)—which are the dopants for PEDOT—and poly(diallyldimethylammonium chloride) (PDADMAC; average Mw = 400,000−500,000, Sigma-Aldrich, USA) and sodium chloride (NaCl: >99.5%, Sigma-Aldrich, USA). Phosphate-buffered saline (PBS; FUJIFILM Wako Pure Chemical Corporation, Japan), associated with *in vivo* operations, was also used as a replacement solution. The molecular structures of these substances are described in Supporting Information S-1. A pair of gold electrodes with a tip radius of 50 μm and a gap of 100 μm was prepared by depositing a 190 nm gold layer with a 10 nm chromium intermediate layer on a glass substrate using EB1100 (Canon Anelva, Japan) as an electrode substrate. Before the experiment, the substrates were cleaned with *N*,*N*-dimethylformamide, acetonitrile, and ethanol to remove surface contaminants and then dried.

Experimental Setup. Figure 1a shows a schematic of the experimental setup used for fabricating the PEDOT:PSS wire via electropolymerization and the subsequent conductance measurements. Detailed information regarding the setup is described in a previous study.[12] The setup was designed to alternately apply an arbitrary input voltage and a measurement voltage (−0.005 V) to the working electrode. The counter electrode was connected to the ground during the input voltage application and then switched to an operational amplifier (op-amp)-based current−voltage converting circuit with an amplification factor of 2.0×10^6 during the measurement voltage application. This arrangement allowed the conversion of the current flowing through the electrodes into a voltage amplified by a factor of 2×10^6 V. An Arduino Mega 2560 was used to control the mechanical relay, which regulated the timing of the input/measurement voltage application and ground/op-amp switching and detected the voltage from the op-amp. The input DC voltage was set with a pulse width of 10 ms and a pulse-to-pulse interval of 800 ms. The measurement DC voltage (−0.005 V) was applied during the interval of the input voltage. To eliminate the effect of ion current on the conductance values, the average conductance between 500 and 750 ms after the application of the measurement voltage was adopted (for a detailed explanation, see Supporting Information S-2).

Method of Fabricating and Evaluating a Synaptic PEDOT:PSS Wire. The synaptic PEDOT:PSS wire was fabricated as follows. Initially, 20 μL of an EDOT + PSS solution was dropped on the electrodes; then, a square-wave AC voltage of 10 Vp−p at 20 kHz was applied to initiate the growth of PEDOT:PSS wires from both electrodes. Once targeted numbers of wires of PEDOT:PSS were connected, the application of the AC voltage was stopped. Figure 1b provides a schematic of the subsequent experimental procedure and the resulting conductance change. To induce synaptic conductance changes in the PEDOT:PSS wire, a DC pulse voltage of +2.5 V, which is larger than the polymerization potential, was applied to the wire. Note that except for the experiment on "Controllability of conductance of PEDOT:PSS wire", we applied the DC pulse 20 times. The applied pulse resulted in a selective increase in the diameter of the PEDOT:PSS wire at the anode due to additional polymerization, which increased the conductance. This operation is called "forming" of the PEDOT:PSS wire, which allows the wire to show synaptic conductance changes when subjected to DC pulse voltages smaller than the polymerization potential. Herein, the measurement of synaptic conductance change involved four repetitions of alternately applying −1 V for 50 pulses and then +1 V for 50 pulses. The applied potential was determined based on cyclic voltammetry (CV) and electrochemical impedance spectroscopy (EIS) measurements of the PEDOT:PSS wire (for a detailed explanation, see Supporting Information S-3). We confirmed that this synaptic conductance change requires both forming the wire and establishing wire connections between the electrodes (for a detailed explanation, see Supporting Information S-2). Except the experiment on controllability of conductance of PEDOT:PSS wires, after the initial measurement of the synaptic conductance change in the EDOT + PSS solution, the solution was replaced with an electrolyte solution through the following processes: the EDOT + PSS solution was removed, and the wire was rinsed twice with 20 μL of acetonitrile. A cylinder made of polydimethylsiloxane (PDMS) with a hollow of φ 5 mm was placed such that the center of the cylinder aligned with the electrode gap and filled with 60 μL of the substitute solution. The PDMS cylinder was then covered with a cover glass to prevent evaporation. In the postsubstitution experiment, the measurement of synaptic conductance changes was followed by a retention measurement, during which only the measurement voltage was applied for 3300 s. Afterward, the polarity of the applied DC pulse voltage was reversed (+1 V for 50 pulses, and then −1 V for 50 pulses), and the synaptic conductance change and retention characteristics were measured again. These experiments were performed in triplicate for each dopant/electrolyte solution, and the average of the data was used to evaluate the full switching window and retention characteristics.

Scanning Electron Microscopy (SEM) Analysis. A SEM (Hitachi High-Tech Corporation SU6600 scanning electron microscope) was used to record images of the PEDOT:PSS wire. SEM images of the wire prepared using the abovementioned procedures were obtained prior to replacing the EDOT + PSS solution with electrolyte solutions. The analysis was conducted at an accelerating voltage of 6 kV and an emission current of 1.8 μA.

DFT Calculation. Gaussian 09 software was used for DFT calculations.[18] Structural optimization was performed using unrestricted B3LYP/6-31++G(d,p), and the energies for each electron system and ion volume were calculated at the unrestricted B3LYP/6-311++G(d,p) level of theory. For B3LYP/6-31++G(d,p) and B3LYP/6-311++G(d,p), the convergence condition and calculation grid were set to "self-consistent field = tight" and "integration = ultrafine," respectively. η served as a parameter to characterize the electrolyte ions and was obtained using the following equations:[19,20]

$$\eta = \frac{1}{2}\left(\frac{\partial^2 E}{\partial N^2}\right) \approx \frac{E_{N+1} - 2E_N + E_{N-1}}{2} = \frac{1}{2}(IP - EA) \quad (1)$$

$$IP = (E_{N-1} - E_N),\ EA = (E_N - E_{N+1}) \quad (2)$$

where E denotes the energy of the ion molecule, N represents the number of electrons, IP denotes the ionization energy, EA represents the electron affinity, E_N denotes the energy of the N-electron system, E_{N+1} represents the energy in the reduced state, and E_{N-1} denotes the energy in the oxidized state. After structural optimization, E_N, E_{N-1}, and E_{N+1} were calculated for each electrolyte ion, yielding η.

RESULTS AND DISCUSSION

Controllability of Conductance of PEDOT:PSS Wires. To confirm the controllability of the conductance of the PEDOT:PSS wires, we examined the effects of the forming conditions of the PEDOT:PSS wires and the number of connected wires on the synaptic device characteristics. Figure 2a shows the results of the synaptic conductance change of the PEDOT:PSS single wires when the number of DC pulses used for forming was varied. The results revealed that the overall conductance and switching range of the conductance increased

https://doi.org/10.1021/acsami.4c12037
ACS Appl. Mater. Interfaces 2024, 16, 54636−54644

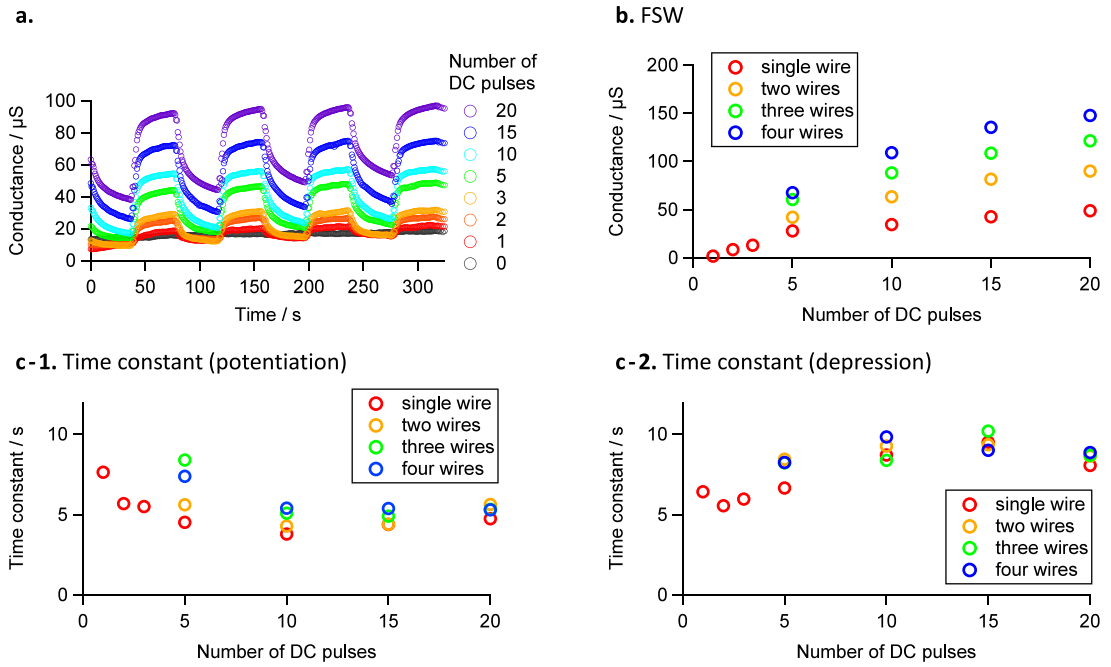

Figure 2. (a) Synaptic conductance change behavior of the PEDOT:PSS single wires fabricated with varying numbers of DC pulses for forming, and the dependence of (b) the FSW and time constant at (c-1) potentiation and (c-2) depression on the number of DC pulses for forming and the number of wires connected between the electrodes.

with an increase in the number of DC pulses used for forming. The unformed PEDOT:PSS wire showed no synaptic conductance changes (see Supporting Information S-2). To establish the characteristics as a synaptic device, we first evaluated the full switching window (FSW). For a detailed definition of the FSW, see Supporting Information S-4. Figure 2b shows the relationship between the FSW, number of DC pulses, and number of connected wires. For the data of the synaptic conductance change behavior, see Supporting Information S-5. The FSW tends to increase with an increase in the number of DC pulses and the number of connected wires. Subsequently, to evaluate the waveforms quantitatively, the synaptic conductance change behavior was fitted using an exponential function, and the time constant (τ) was calculated (for a detailed definition of τ, see Supporting Information S-6). Herein, τ depends on the duration, interval, and number of input pulses, making it a valuable evaluation index for the waveform. A small τ value indicates rapid potentiation/depression of the conductance and a close-to-rectangular (nonlinear) waveform, whereas a large τ value indicates a slow conductance change and a triangular (linear) waveform. Figure 2c-1 and c-2 shows the time constants for potentiation and depression, respectively. When 10−20 DC pulses were applied for forming, regardless of the number of connected wires, the τ value was approximately 5 s for potentiation and 9 s for depression. However, when 1−5 DC pulses were applied, the time constant of potentiation tended to be large, that of depression tended to be small, and the variation in the number of connected wires was large. Therefore, by applying more than 10 DC pulses, stable synaptic conductance change behavior could be obtained, regardless of the number of connected wires. In the following sections, we present the results of forming single PEDOT:PSS wires by applying 20 DC pulses to obtain a large FSW and a stable time constant.

Effect of Ion Species on the Full Switching Window. Figure 3a shows the SEM images of the PEDOT:PSS wire after forming at the anode and cathode sides, revealing a noticeable difference in the wire diameters between the electrodes. The diameters of the PEDOT:PSS wire at the anode and cathode sides were 1.4 and 0.5 μm, respectively. Figure 3b depicts the typical conductance change behavior of the PEDOT:PSS wire during forming and synaptic conductance change measurements in an EDOT + PSS solution. After the initial preparation and measurement, the EDOT + PSS solution was replaced with various electrolyte solutions. Figure 3c shows the synaptic conductance change behavior of the PEDOT:PSS wire in each electrolyte solution, indicating that the PEDOT:PSS wire, after forming, exhibits synaptic conductance change in all electrolyte solutions, regardless of the PEDOT dopant/nondopant. The conductance of the wire in the electrolyte solution depends on the inherent conductance of the PEDOT:PSS wire. Based on the results of the synaptic conductance change, we evaluated the full switching window of the PEDOT:PSS wire quantitatively, according to the rate of change in the full switching window before and after solution substitution (i.e., in the EDOT + PSS and electrolyte solutions, respectively). The rate of change in the full switching window for each electrolyte is summarized in Figure 3d and was found to be dependent on the electrolyte. Notably, all cases exhibit negative rates of change in the full switching window, indicating that the full switching windows in the electrolyte solutions are smaller than those in the EDOT + PSS solution. This decrease in the full switching window is attributed to the difference in the solvents. The change from the cosolvent of acetonitrile and water in the EDOT + PSS solution to water in the electrolyte solution induced a structural change in the PEDOT:PSS wire, decreasing the conductivity and full switching window[21] (for a detailed discussion, see Supporting Information S-7).

Herein, we attempt to explain the relationship between full switching windows and electrolyte ion species based on the hard and soft acids and bases (HSAB) theory.[22] The relationships between the full switching window and the η of

https://doi.org/10.1021/acsami.4c12037
ACS Appl. Mater. Interfaces 2024, 16, 54636−54644

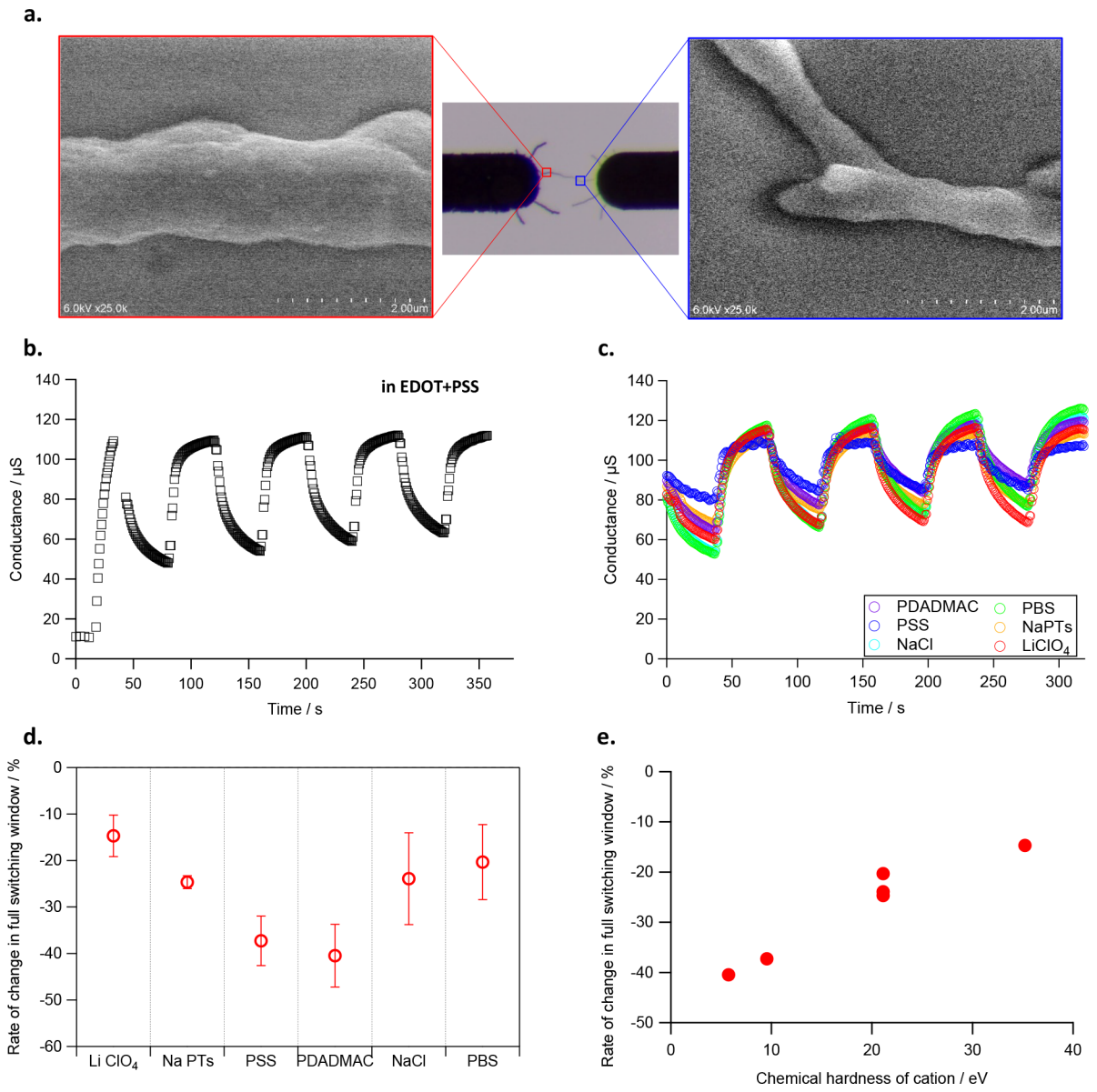

Figure 3. (a) SEM images of the PEDOT:PSS wire after forming at the anode side (red) and the cathode side (blue). (b) Typical conductance behavior of the PEDOT:PSS wire in the EDOT + PSS solution before this solution was replaced with electrolyte solutions. (c) Synaptic conductance change behavior of the PEDOT:PSS wire in various electrolyte solutions. (d) Rate of change in the full switching window of synaptic conductance changes. (e) Relationship between the η of cations and the rate of change in the full switching window.

cations, as obtained through DFT calculations (Figure 3e), indicates that cations with higher η values exhibit a wider full switching window (for specific values of η of the electrolyte ions, see Supporting Information S-8). Notably, the relationship between the rate of change in the dynamic range and the η of the cations shows the same tendency as that between the full switching window and the η of the cations (for a detailed definition of the rate of change in the dynamic range and specific results, see Supporting Information S-9). By contrast, the PSS^- anion, which compensates for the $PEDOT^+$ charge in the PEDOT:PSS wire, shows the lowest η value of 3.41 among the investigated electrolyte anions. Therefore, the PSS^- anions tend to form stable orbital bonds with the cations exhibiting lower η.[23,24]

To further elucidate the abovementioned results, we investigated the mechanism of synaptic conductance change in the PEDOT:PSS wire. A previous study explained the mechanism of synaptic conductance change by reporting that the asymmetric diameter of the PEDOT:PSS wire causes varying efficiencies in doping and dedoping reactions, resulting in a change in the total number of carriers within the wire.[12] Therefore, our focus shifted to the efficiency of the doping/dedoping reactions. In electrolyte solutions, the following redox phenomena are anticipated to occur.[25−27] At the anode, $PEDOT^0$ is oxidized to $PEDOT^+$, and PSS^- compensates and stabilizes the charge of $PEDOT^+$ (doping reaction). Simultaneously, at the cathode, the $PEDOT^+$ (polaron) state is reduced to $PEDOT^0$ (dedoping reaction), and electrolyte cations approach the electrode owing to Coulombic attraction, forming ion pairs with PSS^- to compensate for the charge. These reactions are expressed as follows:

$$PEDOT^+ : PSS^- + X^+ + e^- \rightleftarrows PEDOT^\circ + X^+ : PSS^- \quad (3)$$

https://doi.org/10.1021/acsami.4c12037
ACS Appl. Mater. Interfaces 2024, 16, 54636−54644

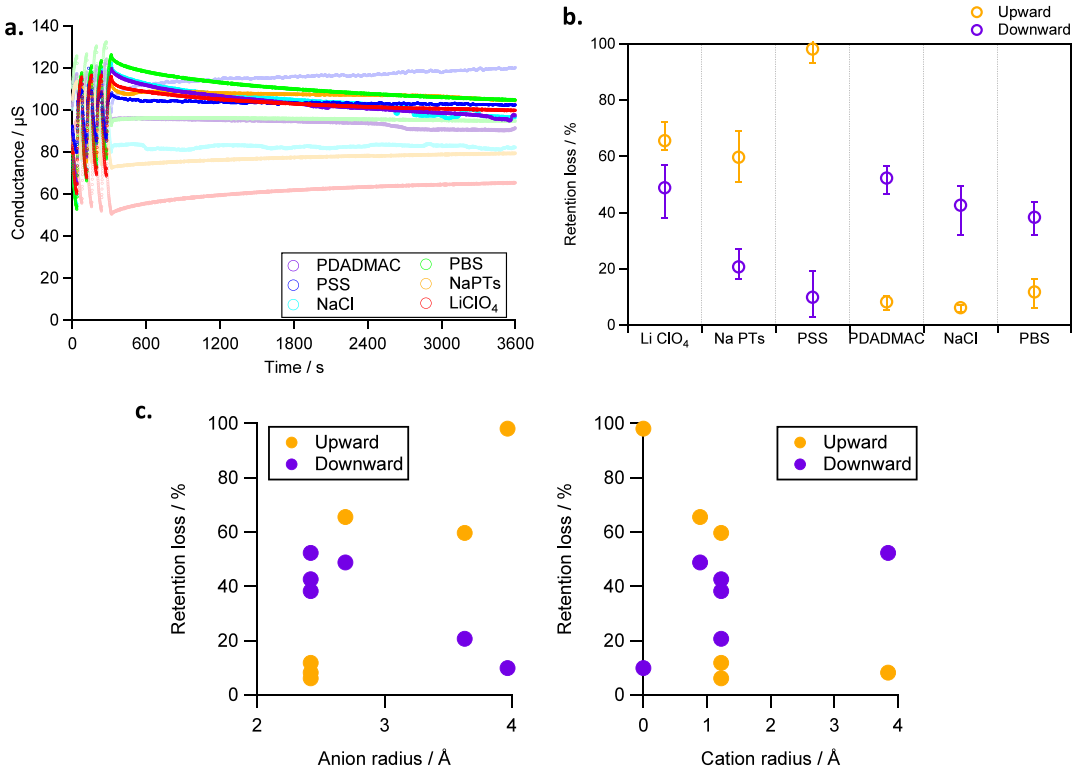

Figure 4. (a) Retention behavior of the PEDOT:PSS wire in various electrolyte solutions. (b) Evaluation of the retention property for each electrolyte. (c) Relationship between the radius of ions and the extent of retention loss.

where X^+ is the electrolyte cation in the aqueous solution. In the doping reaction, the presence of a cation X^+ with a low η value (i.e., high affinity toward PSS^-) leads to the formation of the stable ionic pair X^+:PSS^-. Consequently, the oxidation process of PEDOT requires energy to dissociate the stable ionic pair X^+:PSS^-, increasing the activation energy of the transition from $PEDOT^0$ to $PEDOT^+$ and inhibiting the doping reaction. Inhibition of the doping reaction reduces the number of $PEDOT^+$:PSS^- products, which are the reactants in the reverse dedoping reaction. Hence, the dedoping reaction was also inhibited because of the small number of reactants. According to this mechanism, the full switching window decreases for the cations with low η values.

Effect of Ion Species on Retention Property. Figure 4a shows the retention behavior of the PEDOT:PSS wire in various electrolyte solutions after the synaptic conductance change was measured. The retention characteristics were evaluated based on the retention loss relative to the full switching window. For a detailed definition of retention loss, please refer to Supporting Information S-10. Figure 4b shows the retention loss for each electrolyte solution. The labels "Upward" and "Downward" in Figure 4b represent the direction of retention loss (increase and decrease, respectively), depending on the conductive state of the PEDOT:PSS wire immediately before the retention measurement. In the "Upward" cases, retention starts with low conductance, i.e., the last input pulse of the synaptic conductance measurement is −1 V, and the retention deteriorates along the direction of conductance increase. Conversely, in the "Downward" cases, retention starts with high conductance, and the retention deteriorates along the direction of conductance decrease. The results shown in Figure 4b indicate that the retention loss depends on the electrolyte species. Figure 4c shows the relationship between the retention loss and the cationic and anionic radii (for specific values of the radii of the electrolyte ions, see Supporting Information S-11). Larger anionic radii and smaller cationic radii lead to greater retention loss in the "Upward" cases and smaller retention loss in the "Downward" cases, indicating that during the retention process, electrolyte solutions containing large anions and small cations tend to exhibit a high-resistivity state (HRS), whereas those containing small anions and large cations tend to exhibit a low-resistivity state (LRS). Considering the phenomenon of conductance change based on the asymmetric PEDOT:PSS wire, a thicker wire, in which additional PEDOT:PSS molecules can contribute to the redox reaction, predominantly influences the retention. Therefore, moving forward, we focus on the phenomena occurring at the thicker wire, specifically the anode in the "Downward" cases and the cathode in the "Upward" cases.

First, we discuss the factors contributing to the HRS during the retention process. Before retention, the doped/undoped structure of the PEDOT:PSS wire was determined by applying an external electric field immediately prior to the retention measurement. During retention, the loss of this driving force, that is, the external electric field, may allow the structural relaxation of the PEDOT:PSS wire induced by the hydration of the PSS matrix, enabling conformational changes via hydration. A previous study on PEDOT:PSS films reported that hydrophilic PSS absorbs water under humid conditions, causing structural instability.[28] In fact, Raman spectroscopic measurements revealed that immersing a PEDOT:PSS wire in water causes the dedoping of PEDOT (for a detailed discussion, see Supporting Information S-7). This structural relaxation unbinds some of the $PEDOT^+$:PSS^- pairs, and the unpaired polaron $PEDOT^+$ is converted into $PEDOT^0$,

https://doi.org/10.1021/acsami.4c12037
ACS Appl. Mater. Interfaces 2024, 16, 54636−54644

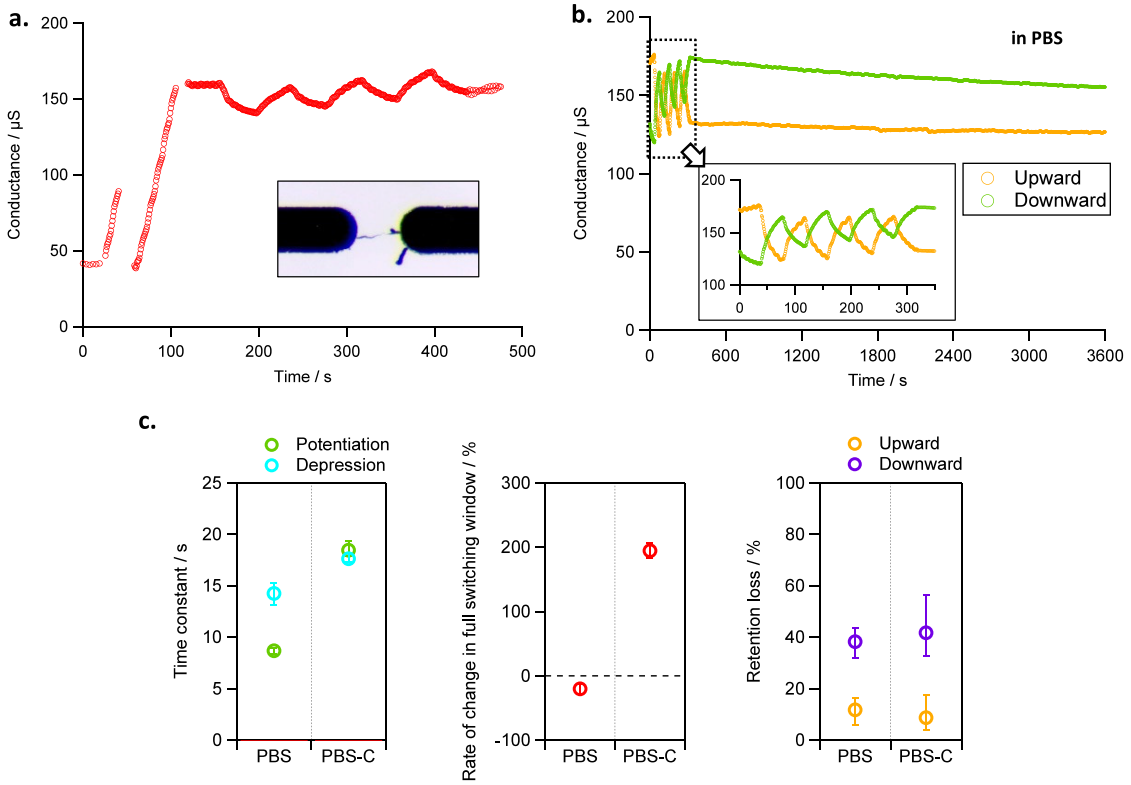

Figure 5. (a) Conductance change in the PEDOT:PSS wire with forming (+2.5 V; 20 pulses) and counter forming (−2.5 V; 60 pulses) observed in the EDOT + PSS solution. (b) Synaptic conductance change of the PEDOT:PSS wire in PBS after forming (+2.5 V; 20 pulses) and counter forming (−2.5 V; 60 pulses). (c) Comparison of the time constant, rate of change in the full switching window, and retention loss of the PEDOT:PSS wires in PBS between forming (+2.5 V; 20 pulses) alone—labeled PBS—and forming (+2.5 V; 20 pulses) and counter forming (−2.5 V; 60 pulses), labeled PBS-C.

decreasing the number of carriers and causing low conductivity. Subsequently, the factors contributing to the LRS during retention are discussed, assuming that anion-exchange doping occurs. Yamashita et al. reported the anion-exchange doping of poly(2,5-bis(3-tetradecylthiophen-2-yl)thieno[3,2-*b*]thiophene) (PBTTT)-conducting polymer films[20] using mixed solutions of organic salts and a tetrafluorotetracyanoquinodimethane dopant. They showed efficient anion-exchange doping using anions with large ionic radii and cations with small ionic radii. Anions with large ionic radii, which afford delocalized charges and poor affinity for small cations, predominantly couple with the delocalized charges on PBTTT. Therefore, electrolyte anions with high affinity (i.e., large ionic radii) interact with polarons of PEDOT instead of PSS when hydration causes PSS^- to separate from $PEDOT^+$. Additionally, small cations interact predominantly with localized PSS^--charged sites. Considering these factors, the conductance during retention is determined based on the balance of structural relaxation induced by the hydration of PSS^- and anion-exchange doping. When large anions and small cations are present, anion-exchange doping and structural relaxation affect the retention, leading to LRS. Conversely, in the presence of small anions and large cations, structural relaxation dominates, resulting in the HRS. Based on this mechanism, achieving a state without retention loss is challenging. However, the use of an electrolyte (e.g., NaCl) that exhibits moderate retention in the downward and upward retention processes can minimize the influence of retention.

Optimization of Conductance Change Behavior in the PBS Solution. As shown in Figure 3c, the conductance changes nonlinearly with an increasing number of input pulses. Nonlinear conductance change behavior in synaptic devices can lead to poor convergence during learning, resulting in a loss of training accuracy.[29,30] Therefore, controlling the waveform of the conductance change is desirable for the practical application of these devices. Herein, we explored the use of forming, by which the diameter of the PEDOT:PSS wire between electrodes becomes asymmetric, to achieve a synaptic conductance change, and hypothesized that additional forming of the PEDOT:PSS wire at the counter electrode could control the doping efficiency and waveform of the conductance change. Counter forming, which involves the application of voltage with a reverse polarity to normal forming, was applied to achieve this goal. Figure 5a shows the synaptic conductance change behavior of the PEDOT:PSS wire treated with forming (+2.5 V; 20 pulses) and counter forming (−2.5 V; 60 pulses) in the EDOT + PSS solution. The application of counter forming afforded a triangular waveform, indicating linear changes in conductance compared to forming alone (Figure 3b); the polarity of the synaptic conductance change was reversed, and the full switching window decreased. After the experiment shown in Figure 5a, the EDOT + PSS solution was replaced with PBS, and the synaptic conductance change was measured (Figure 5b). The results showed that the synaptic conductance change behavior of the triangular waveform was maintained even after solution replacement.

In Figure 5c, the time constant, rate of change in full switching window, and retention loss are compared for the case of forming alone (+2.5 V; 20 pulses) and the case of forming (+2.5 V; 20 pulses) and counter forming (−2.5 V; 60 pulses).

https://doi.org/10.1021/acsami.4c12037
ACS Appl. Mater. Interfaces 2024, 16, 54636−54644

The results showed that counter forming increased the time constant and improved the waveform from nonlinear to linear. Furthermore, counter forming reduced the difference in the time constant between the potentiation/depression processes, representing the acquisition of a symmetrical waveform advantageous for mechanical learning.[29,31] Interestingly, the rate of change in the full switching window increased considerably with the application of counter forming, indicating that although counter forming induced a decrease in the full switching window in the EDOT + PSS solution (Figure 5a), it expanded the full switching window when the wire was operated in PBS. Although the difference regarding the retention loss was not remarkable, the retention during the "Upward" case was suppressed. These results indicate that the conductance change behavior suitable for learning can be achieved by applying counter forming and maintaining the wire in the PBS solution.

CONCLUSIONS

Herein, we investigated the effects of electrolyte ions on the synaptic functions of PEDOT:PSS wires and discussed their contribution mechanisms. The synaptic conductance change in the PEDOT:PSS wire treated with forming was induced by electrolyte ions, and the full switching window and retention properties were closely related to the properties of the electrolytes. Electrolyte cations with low η values, displaying a high affinity for PSS^-, led to a decrease in the full switching window. During retention, electrolyte solutions with large anions and small cations tended to exhibit the HRS, whereas those with small anions and large cations tended to exhibit the LRS. Therefore, the performance of the PEDOT:PSS wire as a synaptic device is highly dependent on the ionic species of the electrolyte, necessitating a careful selection of the operating environmental conditions. Furthermore, the synaptic conductance change waveform can be controlled by adjusting the forming conditions and maintaining the device in a PBS solution. Finally, this study demonstrated that the PEDOT:PSS wire functions as a synaptic device in electrolyte solutions, including PBS, and can exhibit a linear change in conductance, which is favorable for learning, by adjusting the forming conditions. Unlike the three-terminal PEDOT thin-film devices reported in previous studies,[6,32] the two-terminal device based on PEDOT wires requires little space. Moreover, our previous study demonstrated three-dimensional wiring of a PEDOT wire.[13] These facts indicate the potential of the PEDOT wire, which may pave the way for the development of novel integrated synaptic devices. The compact design is also an advantage when placing elements in a limited space, such as inside the human body. In addition, PEDOT:PSS is a biocompatible material. Therefore, PEDOT:PSS wires are promising materials for use in two-terminal synaptic devices that can be applied in clinical studies.

Combining PEDOT:PSS synaptic devices with reservoir devices may realize an innovative neuromorphic architecture, enabling *in vivo* information processing with intelligent logic, such as pulse sensors capable of autonomously determining the required information and initiating communication only when necessary. This advancement is promising for the development of advanced neuromorphic hardware with a wide array of potential applications.

ASSOCIATED CONTENT

Supporting Information

The Supporting Information is available free of charge at https://pubs.acs.org/doi/10.1021/acsami.4c12037.

Molecular structure of chemicals; effect of forming and connection of PEDOT:PSS wire; cyclic voltammetry (CV) measurements and electrochemical impedance spectroscopy (EIS) of PEDOT:PSS wire; definition of the rate of change in the full switching window; synaptic conductance change depending on the numbers of forming pulses and connection wires; definition of time constant; effect of solvent/cosolvent on the full switching window; the value of chemical hardness η of electrolyte ions; definition of the rate of change in the dynamic range; definition of retention loss; sizes of electrolyte ions; synaptic conductance change of the PEDOT:PSS wire in PBS after forming only; relationship between molecular properties and synaptic properties; switching durability of PEDOT:PSS wire; and comparison of NaCl and PBS (PDF)

AUTHOR INFORMATION

Corresponding Author

Seiya Watanabe − *Graduate School of Science, Department of Chemistry, Osaka University, Toyonaka, Osaka 560-0043, Japan;* orcid.org/0000-0001-7422-8452; Email: s-watanabe.sci@osaka-u.ac.jp

Authors

Hiroaki Shibakita − *School of Science, Department of Physics, Osaka University, Toyonaka, Osaka 560-0043, Japan*

Naruki Hagiwara − *Graduate School of Information Science & Technology (IST), Hokkaido University, Sapporo, Hokkaido 060-0814, Japan*

Ryosuke Nakajima − *Graduate School of Science, Department of Chemistry, Osaka University, Toyonaka, Osaka 560-0043, Japan*

Hiroyuki S. Kato − *Graduate School of Science, Department of Chemistry, Osaka University, Toyonaka, Osaka 560-0043, Japan;* orcid.org/0000-0002-7663-9404

Megumi Akai-Kasaya − *Graduate School of Science, Department of Chemistry, Osaka University, Toyonaka, Osaka 560-0043, Japan; Faculty of Information Science & Technology (IST), Hokkaido University, Sapporo, Hokkaido 060-0814, Japan*

Complete contact information is available at: https://pubs.acs.org/10.1021/acsami.4c12037

Author Contributions

The manuscript was written with contributions from all authors. All authors approved the final version of the manuscript. S.W. designed the study, wrote the manuscript, and collected and analyzed the data. H.S. and N.H. assisted with the data collection. R.N. and H.S.K. aided in interpreting the data. M.A.-K. designed the main concepts and supervised the study.

Funding

This work was supported by the JST CREST Grant Number JPMJCR21B5.

Notes

The authors declare no competing financial interest.

■ ACKNOWLEDGMENTS

Part of this work was supported by the "Nanotechnology Platform Project (Nanotechnology Open Facilities at Osaka University)" of the Ministry of Education, Culture, Sports, Science and Technology, Japan (MEXT) [Grant No.: JPMXP1222OS1039]. The SEM measurements were performed at the Analytical Instrument Facility, Graduate School of Science, Osaka University.

■ REFERENCES

(1) Christensen, D. V.; Dittmann, R.; Linares-Barranco, B.; Sebastian, A.; Le Gallo, M.; Redaelli, A.; Slesazeck, S.; Mikolajick, T.; Spiga, S.; Menzel, S.; et al. 2022 roadmap on neuromorphic computing and engineering. *Neuromorphic Computing and Engineering* **2022**, *2* (2), No. 022501.

(2) Markovic, D.; Mizrahi, A.; Querlioz, D.; Grollier, J. Physics for neuromorphic computing. *Nature Reviews Physics* **2020**, *2* (9), 499−510.

(3) Jo, S. H.; Chang, T.; Ebong, I.; Bhadviya, B. B.; Mazumder, P.; Lu, W. Nanoscale Memristor Device as Synapse in Neuromorphic Systems. *Nano Lett.* **2010**, *10* (4), 1297−1301.

(4) Ohno, T.; Hasegawa, T.; Tsuruoka, T.; Terabe, K.; Gimzewski, J. K.; Aono, M. Short-term plasticity and long-term potentiation mimicked in single inorganic synapses. *Nat. Mater.* **2011**, *10* (8), 591−595.

(5) Wang, Z. R.; Joshi, S.; Savel'ev, S. E.; Jiang, H.; Midya, R.; Lin, P.; Hu, M.; Ge, N.; Strachan, J. P.; Li, Z. Y.; et al. Memristors with diffusive dynamics as synaptic emulators for neuromorphic computing. *Nat. Mater.* **2017**, *16* (1), 101−108.

(6) Van de Burgt, Y.; Lubberman, E.; Fuller, E. J.; Keene, S. T.; Faria, G. C.; Agarwal, S.; Marinella, M. J.; Alec Talin, A.; Salleo, A. A non-volatile organic electrochemical device as a low-voltage artificial synapse for neuromorphic computing. *Nat. Mater.* **2017**, *16* (4), 414−418.

(7) Wang, H.; Zhao, Q.; Ni, Z.; Li, Q.; Liu, H.; Yang, Y.; Wang, L.; Ran, Y.; Guo, Y.; Hu, W.; et al. A Ferroelectric/Electrochemical Modulated Organic Synapse for Ultraflexible, Artificial Visual-Perception System. *Adv. Mater.* **2018**, *30* (46), No. 1803961.

(8) Ji, X.; Paulsen, B. D.; Chik, G. K. K.; Wu, R.; Yin, Y.; Chan, P. K. L.; Rivnay, J. Mimicking associative learning using an ion-trapping non-volatile synaptic organic electrochemical transistor. *Nat. Commun.* **2021**, *12* (1), 2480.

(9) Cho, Y. U.; Lee, J. Y.; Jeong, U. J.; Park, S. H.; Lim, S. L.; Kim, K. Y.; Jang, J. W.; Park, J. H.; Kim, H. W.; Shin, H.; et al. Ultra-Low Cost, Facile Fabrication of Transparent Neural Electrode Array for Electrocorticography with Photoelectric Artifact-Free Optogenetics. *Adv. Funct. Mater.* **2022**, *32* (10), No. 2105568.

(10) Qiang, Y.; Artoni, P.; Seo, K. J.; Culaclii, S.; Hogan, V.; Zhao, X.; Zhong, Y.; Han, X.; Wang, P. M.; Lo, Y. K.; et al. Transparent arrays of bilayer-nanomesh microelectrodes for simultaneous electrophysiology and two-photon imaging in the brain. *Sci. Adv.* **2018**, *4* (9), No. eaat0626.

(11) Terutsuki, D.; Yoroizuka, H.; Osawa, S. I.; Ogihara, Y.; Abe, H.; Nakagawa, A.; Iwasaki, M.; Nishizawa, M. Totally Organic Hydrogel-Based Self-Closing Cuff Electrode for Vagus Nerve Stimulation. *Adv. Healthcare Mater.* **2022**, *11* (23), No. 2270142.

(12) Hagiwara, N.; Sekizaki, S.; Kuwahara, Y.; Asai, T.; Akai-Kasaya, M. Long- and Short-Term Conductance Control of Artificial Polymer Wire Synapses. *Polymers* **2021**, *13* (2), 312.

(13) Hagiwara, N.; Asai, T.; Ando, K.; Akai-Kasaya, M. Fabrication and Training of 3D Conductive Polymer Networks for Neuromorphic Wetware. *Adv. Funct. Mater.* **2023**, *33*, 2300903.

(14) Cucchi, M.; Gruener, C.; Petrauskas, L.; Steiner, P.; Tseng, H.; Fischer, A.; Penkovsky, B.; Matthus, C.; Birkholz, P.; Kleemann, H.; et al. Reservoir computing with biocompatible organic electrochemical networks for brain-inspired biosignal classification. *Sci. Adv.* **2021**, *7* (34), No. eabh0693.

(15) Tanaka, G.; Yamane, T.; Heroux, J. B.; Nakane, R.; Kanazawa, N.; Takeda, S.; Numata, H.; Nakano, D.; Hirose, A. Recent advances in physical reservoir computing: A review. *Neural Networks* **2019**, *115*, 100−123.

(16) Nakajima, K. Physical reservoir computing-an introductory perspective. *Jpn. J. Appl. Phys.* **2020**, *59* (6), No. 060501.

(17) Milano, G.; Pedretti, G.; Montano, K.; Ricci, S.; Hashemkhani, S.; Boarino, L.; Ielmini, D.; Ricciardi, C. In materia reservoir computing with a fully memristive architecture based on self-organizing nanowire networks. *Nat. Mater.* **2022**, *21* (2), 195−202.

(18) *Gaussian 09 Rev. A.02*; Wallingford, CT, 2016. (accessed.

(19) Jonsson, E.; Johansson, P. Electrochemical oxidation stability of anions for modern battery electrolytes: a CBS and DFT study. *Phys. Chem. Chem. Phys.* **2015**, *17* (5), 3697−3703.

(20) Yamashita, Y.; Tsurumi, J.; Ohno, M.; Fujimoto, R.; Kumagai, S.; Kurosawa, T.; Okamoto, T.; Takeya, J.; Watanabe, S. Efficient molecular doping of polymeric semiconductors driven by anion exchange. *Nature* **2019**, *572* (7771), 634.

(21) Xia, Y. J.; Ouyang, J. Y. PEDOT:PSS films with significantly enhanced conductivities induced by preferential solvation with cosolvents and their application in polymer photovoltaic cells. *J. Mater. Chem.* **2011**, *21* (13), 4927−4936.

(22) Pearson, R. G. Hard and soft acids and bases - the evolution of a chemical concept. *Coord. Chem. Rev.* **1990**, *100*, 403−425.

(23) Klopman, G. Chemical reactivity and concept of charge- and frontier-controlled reactions. *J. Am. Chem. Soc.* **1968**, *90* (2), 223.

(24) Chattaraj, P. K. Chemical reactivity and selectivity: Local HSAB principle versus frontier orbital theory. *J. Phys. Chem. A* **2001**, *105* (2), 511−513.

(25) Proctor, C. M.; Rivnay, J.; Malliaras, G. G. Understanding Volumetric Capacitance in Conducting Polymers. *J. Polym. Sci., Part B: Polym. Phys.* **2016**, *54* (15), 1433−1436.

(26) Fabiano, S.; Sani, N.; Kawahara, J.; Kergoat, L.; Nissa, J.; Engquist, I.; Crispin, X.; Berggren, M. Ferroelectric polarization induces electronic nonlinearity in ion-doped conducting polymers. *Sci. Adv.* **2017**, *3* (6), No. e1700345.

(27) Savva, A.; Wustoni, S.; Inal, S. Ionic-to-electronic coupling efficiency in PEDOT:PSS films operated in aqueous electrolytes. *Journal of Materials Chemistry C* **2018**, *6* (44), 12023−12030.

(28) Fan, X.; Nie, W.; Tsai, H.; Wang, N.; Huang, H.; Cheng, Y.; Wen, R.; Ma, L.; Yan, F.; Xia, Y. PEDOT:PSS for Flexible and Stretchable Electronics: Modifications, Strategies, and Applications. *Adv. Sci.* **2019**, *6* (19), No. 1900813.

(29) Zhao, M.; Gao, B.; Tang, J.; Qian, H.; Wu, H. Reliability of analog resistive switching memory for neuromorphic computing. *Appl. Phys. Rev.* **2020**, *7* (1), No. 011301.

(30) Chen, P. Y.; Lin, B.; Wang, I. T.; Hou, T. H.; Ye, J.; Vrudhula, S.; Seo, J. S.; Cao, Y.; Yu, S. Mitigating Effects of Non-ideal Synaptic Device Characteristics for On-chip Learning. In *34th IEEE/ACM International Conference on Computer-Aided Design (ICCAD)*; IEEE: Austin, TX, Nov 02−06, 2015; *2015*; pp 194−199.

(31) Tang, J.; Bishop, D.; Kim, S.; Copel, M.; Gokmen, T.; Todorov, T.; Shin, S.; Lee, K. T.; Solomon, P.; Chan, K.et al. ECRAM as Scalable Synaptic Cell for High-Speed, Low-Power Neuromorphic Computing. In *2018 IEEE International Electron Devices Meeting (IEDM)*; IEEE: 2018.

(32) Battistoni, S.; Peruzzi, C.; Verna, A.; Marasso, S. L.; Cocuzza, M.; Erokhin, V.; Iannotta, S. Synaptic Response in Organic Electrochemical Transistor Gated by a Graphene Electrode. *Flexible Printed Electron.* **2019**, *4* (4), No. 044002.

https://doi.org/10.1021/acsami.4c12037
ACS Appl. Mater. Interfaces 2024, 16, 54636−54644